Geophysical Research Letters

RESEARCH LETTER
10.1029/2020GL091920

Airborne Dust Plumes Lofted by Dislodged Ice Blocks at Russell Crater, Mars

Cynthia L. Dinwiddie[1] and **Timothy N. Titus**[2]

[1]Space Science and Engineering Division, Southwest Research Institute®, San Antonio, TX, USA, [2]U.S. Geological Survey, Astrogeology Science Center, Flagstaff, AZ, USA

Key Points:

- We use thermal models and 11 years of Mars data to characterize seasonal activity, providing insight into formation of linear dune gullies
- We propose that basal sublimation dislodges ice blocks that slide downhill, redistributing sublimation lag into plumes and gully fringes
- We offer a compelling story that vent-dislodged CO_2 ice blocks are a modern agent of change on the Russell crater megadune

Supporting Information:

- Supporting Information S1
- Table S1

Correspondence to:
C. L. Dinwiddie,
cdinwiddie@swri.org

Citation:
Dinwiddie, C. L., & Titus, T. N. (2021). Airborne dust plumes lofted by dislodged ice blocks at Russell crater, Mars. *Geophysical Research Letters*, *48*, e2020GL091920. https://doi.org/10.1029/2020GL091920

Received 1 DEC 2020
Accepted 12 FEB 2021

Abstract Linear dune gullies on poleward-facing Martian slopes are enigmatic. Formation by CO_2-ice block or snow cornice falls has been proposed based on optical imagery of bright, high-albedo features inside gully channels. Because these features often resemble patchy frost residue rather than three-dimensional blocks, more evidence is needed to support the ice-block formation mechanism. Satellite imagery captured two simultaneous airborne plumes with in-channel sources at the Russell crater megadune, thrust up, and dispersed outward along the path of linear dune gullies. We use spectral data analyses, climatic analyses of bolometric temperatures, and thermal modeling to further develop the mechanistic framework for linear dune gully development. Basal sublimation and CO_2 gas venting likely cause CO_2-ice-block detachment and falls from gully alcoves in southern early spring, accompanied by ice-block off-gassing and saltation of sands and coarse silts that are redeposited around gully channels, and lofting of sublimation lag (coarse dust/silt) into airborne plumes.

Plain Language Summary For 2 decades, planetary scientists have had many ideas about how and when very long, narrow gullies formed on frost-affected sand dunes on Mars. First, it was thought that they were remnant features left behind millions of years ago when the climate may have supported a wetter environment. Then, repeat imagery showed that gully changes were occurring in the present day, even though the current climate is extremely arid. More recently, scientists observed bright and discrete ice-like features resting inside gully channels, and proposed that carbon dioxide ice blocks (dry ice) had slid down dunes inside these channels. We present satellite imagery of airborne dust plumes lofted by mobile ice blocks sliding down gullies in 2007, 2012, and 2016, captured by two cameras onboard Mars Reconnaissance Orbiter at nearly the same position in the Martian orbit, demonstrating that the activity is seasonal and predictable. The sliding ice blocks agitate dust resting on the surface, thereby generating easily recognizable billowing plumes of dust. Fine-grained dust is suspended in the atmosphere where it can travel longer distances before settling, whereas coarse-grained dust saltates away from gullies, settles, and forms bright fringes around the dark sand of active gullies.

1. Introduction

On Mars, linear dune gullies (Figure 1) headed by small alcoves or catchments drain into small tributaries that focus erodible material into very long, narrow, sinuous-to-parallel gully channels surrounded by lateral levees (Figure 1a; Auld & Dixon, 2016; Diniega, 2014). Near the gully terminus, channels may be perched upon underlying channel deposits, such that the base of channels is higher than the adjacent dune surface (Jouannic et al., 2015), indicating that nearly invisible, vertically stacked depositional gully aprons may indeed be associated with linear dune gullies. Linear dune gullies are documented between 36.3° and 70.4°S (Pasquon et al., 2016).

At the Russell crater megadune (54.3°S/12.9°E), ~1,000 km west of the Hellas Basin, repeat optical imagery has established an 11-Mars-year time series for monitoring local seasonal processes. The megadune is barchanoid (Figure S1a), has a 50 km crest length, is 7–11 km wide, and 500 m high (Gardin et al., 2010). Superimposed on its stoss slope are more than a dozen transverse dunes with west-northwest-facing lee slopes (Jouannic et al., 2012; Figure S1a). Hundreds of linear dune gully channels, 3–30 m wide, up to 2.5 km long (Auld & Dixon, 2016) with mean incision depths of 1.5 m (Diniega, 2014; Jouannic et al., 2012) have formed on the poleward, southwest-facing, 5° to >40° lee slope (steep slopes may imply sand cementation). Where the lee slope orientation switches to west-northwest-facing, linear dune gullies are absent (Figure S1a).

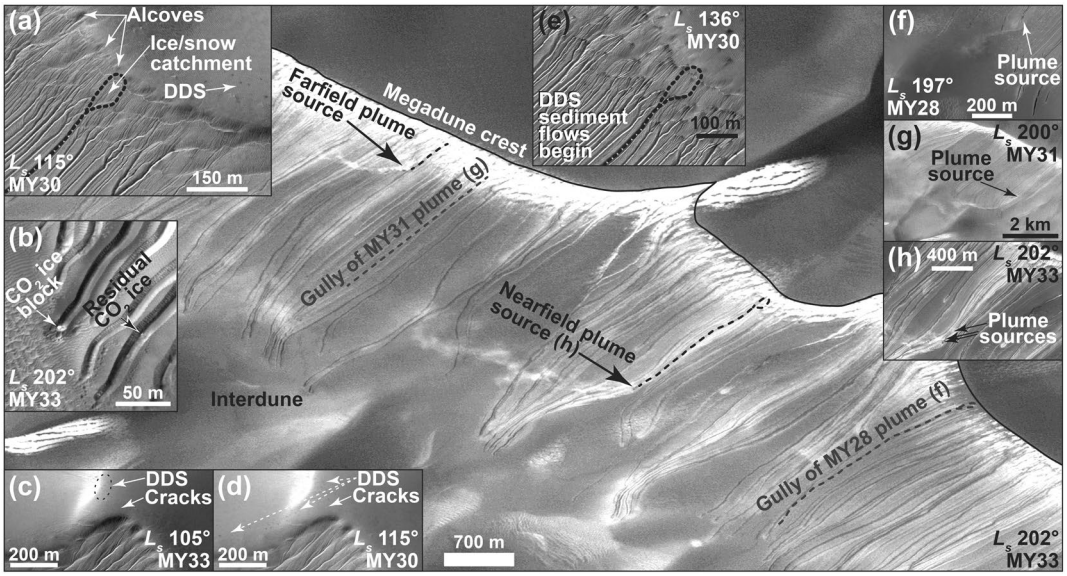

Figure 1. Seasonal processes on the Russell crater megadune culminate with launch of airborne dust plumes by sliding CO_2 ice blocks. Image IDs are as reported in supporting information Tables S1a and S1b. Subparts (a)–(h) are enlarged in supporting information Figure S1. (a) Dense, small tributaries in catchments and gully alcoves connect and funnel material into large linear gully channels; catchment spawning ice block that launched the MY33 near-field plume is indicated; (b) ~5 m CO_2 ice block in a gully channel at L_s 202°; (c) early dark dune spots appear on crest of a secondary dune at L_s 105°; (d) more dark dune spots appear by L_s 115°; (e) dark dune spots annually produce gravitational flows on steep slopes and in small tributaries by L_s 136°; catchment spawning ice block that launched the MY33 near-field plume is indicated; (f) HiRISE image of airborne plume launched at L_s 197° in MY28; (g) CTX image of plume launched at L_s 200° in MY31; (h) HiRISE image of proximal source zone of near-field plume observed in the background CTX image of this figure. CTX Image Credit: NASA/JPL/Malin Space Science Systems; HiRISE Image Credit: NASA/JPL/University of Arizona. CTX, Context Camera; HiRISE, High Resolution Imaging Science Experiment.

Where the slope angle increases above gully channels, scalloped alcoves may occur along the megadune crest; alcoves have median widths and lengths of 27 and 89 m, respectively (Auld & Dixon, 2016; Figure 1a). Where alcoves are absent, other tributary catchments are present at the head of linear dune gullies (Figure S1b). From the upper reaches of alcoves or catchments to the proximal end of distinctly channelized linear gullies, there is a ~170–350-m-long transitional downslope zone where many small tributaries connect before emptying into larger linear dune gullies (Figures 1a and S1b). Below the proximal origin of linear gully channels, ~150–200 m below the dune crest, sinuosity and connections between channels remain significant for another ~150–550 m downslope, beyond which gully sinuosity decreases and channels are generally subparallel (Jouannic et al., 2012). Terminal pits, near the gully terminus but often disconnected from the channels, are frequently observed (Figures 1b and S1c; Jouannic et al., 2012; Pasquon et al., 2016; Reiss & Jaumann, 2003).

Early interpretations of Russell crater linear dune gullies were dominated by a debris-flow hypothesis involving a liquid component made available through thaw of near-surface H_2O ice under high obliquity, no more recently than 6 Ma (Costard et al., 2002; Jouannic et al., 2012; Mangold et al., 2003, 2010; Miyamoto et al., 2004; Reiss et al., 2010; Reiss & Jaumann, 2003). Physical analogue laboratory studies suggested that liquid water may have been released into periglacial debris flows from a seasonally thawing active layer above ice-rich permafrost in the megadune; the permafrost table was thought to control the depth of gully incision (Jouannic et al., 2015; Védie et al., 2008).

Acquisition of new, higher resolution optical data has resulted in year-to-year change detections that demonstrate linear dune gully activity happens annually, under current obliquity (Diniega et al., 2013; Dundas et al., 2012; Reiss & Jaumann, 2003; Reiss et al., 2010). This activity is recent, annual, and occurs when CO_2 frost is sublimating (Gardin et al., 2010; Jouannic et al., 2012, 2015; Pilorget & Forget, 2016; Reiss et al., 2010). Perennial rill systems and recurrent diffusing flows on the megadune lee slope cause annual

morphologic change each spring (Jouannic et al., 2012, 2018; Pasquon et al., 2016; Reiss et al., 2010). Compact Reconnaissance Imaging Spectrometer for Mars (CRISM) observations indicate that CO_2 ice is the prevalent surface volatile from autumn through early spring with trace amounts of H_2O ice (Ceamanos et al., 2011; Gardin et al., 2010; Jouannic et al., 2018; Reiss et al., 2010). Near the end of the frosted season, apparent residual bright frost is present in linear gullies; occasionally high-resolution optical imagery supports the postulate that three-dimensional blocks of bright CO_2 ice sit at rest within the linear dune gullies on the Russell crater megadune (Figures 1b and S1c; Diniega et al., 2013; Dundas et al, 2012, 2019; McKeown et al., 2017). These may be CO_2 ice blocks or cornices that detached and slid downslope, but additional evidence is needed.

We reviewed optical imagery acquired on 183 dates and supplemented these observations with analysis of selected spectral imagery to conduct a comprehensive analysis of the annual timeline for local climate, microclimates, and seasonal processes that yield linear dune gullies at Russell crater, Mars. Location-specific datasets from Thermal Emission Spectrometer (TES; Christensen et al., 1992, 2001), Thermal Emission Imaging System (Christensen et al., 2004), CRISM (Murchie et al., 2007) spectral imagery, and multi-temporal optical imagery from the Narrow Angle Mars Orbiter Camera (Malin et al., 1992; 2010), the Context Camera (CTX; Malin et al., 2007), and the High Resolution Imaging Science Experiment (HiRISE; McEwen et al., 2007) were analyzed (see Text S2 for details).

2. Cold Season Site Characterization

In optical imagery, frost is observed to initially condense on the megadune between solar longitude (L_s) 30° and 40° each year (Figures 2 and 3a). Modeled CO_2 ice thickness on the megadune, as a function of L_s and slope angle (Figures 2 and S2c), as estimated from the KRC thermal model (Kieffer, 2013; see Text S2), is consistent with optical observations of first frost. Frost deposition begins first on the steepest poleward-facing

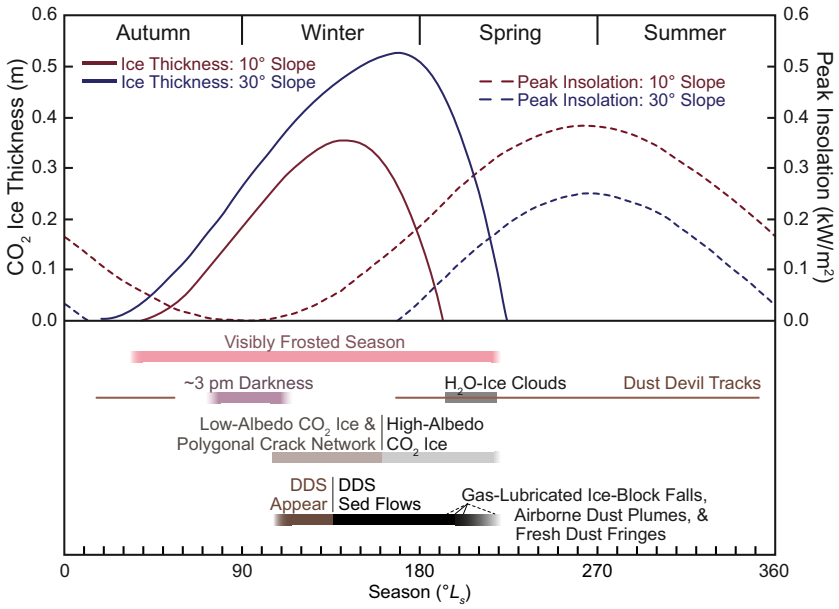

Figure 2. Timeline of seasonal activity at Russell crater, Mars. Pink bar illustrates when the landscape appears frosted in optical imagery. Thin, brown bars indicate dust-devil season. Lavender bar illustrates afternoon darkness, after which dark dune spots (DDS: inferred Kieffer vents) appear and evolve (brown bar). CO_2 ice is translucent and a polygonal crack network is initially observed in the ice on certain slopes (taupe bar). Sediment flows from DDS begin in mid-winter and continue until ice thickness no longer supports venting and resealing mechanisms. As insolation increases, CO_2 ice brightens significantly (light gray bar), and the polygonal crack network is no longer visible, although inferred to remain present. Inferred H_2O ice clouds are observed in early to mid-spring (dark gray bar), near the end of the defrosting season. Modeled CO_2 ice thickness (estimated from the KRC thermal model assuming a density of 1,000 kg/m^3, see Text S2 and Figure S2 for more details) and peak insolation as functions of solar longitude are presented for poleward-facing 10° and 30° slopes. DDS, dark dune spots.

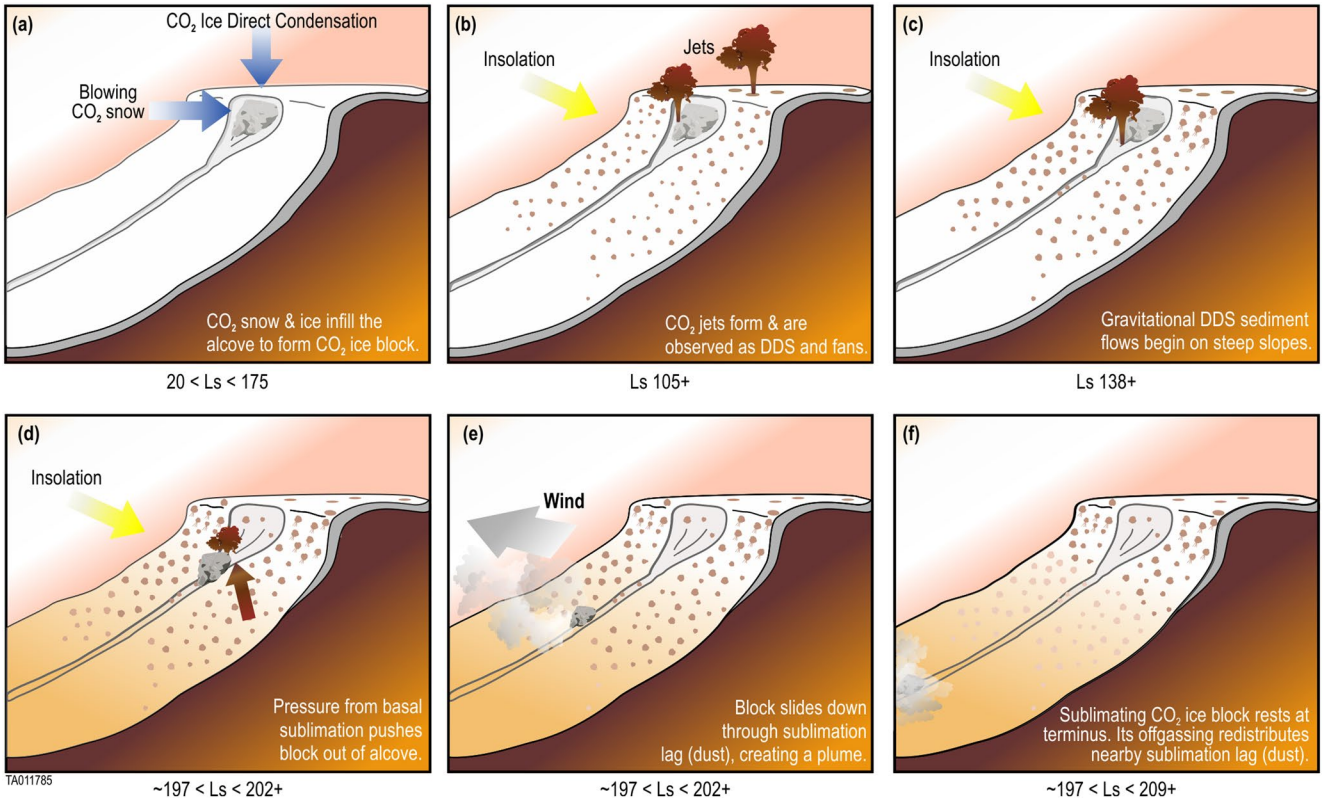

Figure 3. Lifecycle of a CO_2 ice block. (a) Direct condensation of CO_2 ice from the atmosphere and windblown CO_2 snow fill alcoves or catchments; snow anneals and morphs into translucent ice. (b) After a winter period of ~3pm darkness, insolation-induced basal sublimation drives jets of CO_2 gas upward with entrained dune sand and silt, forming dark dune spots (DDS), DDS halos, and windblown fans. (c) DDS vents repeatedly seal and release sediment, and after a period of time, vent-area sediment begins to flow downslope. (d) Ice-brightening occurs, widespread defrosting begins, and translucent CO_2 ice in catchments and alcoves may be agitated, dislodged, and broken out of its in situ slab position by upward CO_2 gas pressure applied by ongoing DDS venting. (e) A dislodged block of high-albedo ice slides downslope and into a linear dune gully channel, through sublimation lag (dust/silt), which forms a visibly opaque plume that is carried by the prevailing wind. (f) The bright ice block comes to rest lower on the slope, near the terminus of an existing gully, and CO_2 gas pressure from the subliming block redistributes coarse dust/silt/sand away from it via saltation, potentially leaving an intermediate-albedo silt fringe around the gully and a low-albedo sand fringe on freshly dust-free gully levees.

slopes, where it also accumulates the thickest deposits that persist into mid-spring (Figure 2), as determined from the KRC thermal model. Model output demonstrates that shallower slopes accumulate thinner blankets of frost later and lose them earlier (Figure 2). Once afternoon daylight returns, faint dark dune spots (DDS; Mangold et al., 2003) appear on the crests of superimposed secondary dunes (Figures 1c, 2, and 3b) as early as L_s 105° (MY33) when (i) 16- to 36-cm-thick frost (model estimate, assuming a CO_2 ice density of 1,000 kg/m^3; see Text S2) has accumulated on pole-facing slopes (Figure S2c), (ii) estimated basal heat flux is <1.9 W/m^2, and (iii) peak insolation absorbed by the ice ranges from 0 W/m^2 on slopes steeper than 11.4° to ~60 W/m^2 on flat plains (Figure S2d).

At L_s 105°, a polygonal crack network is also visible in ~25- to 30-cm-thick (model estimate, Text S2), low-albedo, translucent CO_2 ice (Figures 2 and S2c) on the <25° stoss slope of a superimposed secondary dune. By L_s 115° (MY30; Figure S1i), when 20- to 41-cm-thick (model estimate, Text S2) frost has accumulated on pole-facing slopes (Figure S2c), estimated basal heat flux is <1.35 W/m^2 and peak insolation absorbed by ice ranges from 0 W/m^2 on slopes steeper than 10° to ~78 W/m^2 on flat plains (Figure S2d), and the quantity of visible DDS greatly increases on the megadune crest, in scalloped alcoves along the ridge, on the lee slope, and on stoss slopes of superimposed secondary dunes (Figures 1d and S1i).

It has been proposed that DDS and associated dendritic, araneiform troughs (Gardin et al., 2010; Portyankina et al., 2017), or furrows (McKeown et al., 2017) mark vents of explosively released, high-pressure CO_2 gas jets (i.e., Kieffer's jets; Pilorget & Forget, 2016; Piqueux & Christensen, 2008; Portyankina, 2014) at weak

spots in the CO_2 ice; CO_2 gas forms at the dune–ice interface from basal heat flux or insolation-induced basal sublimation (IIBS) of the translucent ice, or both (Aharonson, 2004; Hansen et al., 2010). Kieffer (2007) provides a detailed description of this venting process, which produces dark fan-shaped deposits of sand above the ice (Malin & Edgett, 2001). By L_s 136° (MY30) (and possibly earlier), DDS vents are producing channelized, gravitational flows of dark sediment when the translucent ice is expected to be >0.4-m-thick based on model estimates (Figures 1e, 2, 3c, S1j, and S2c). Pilorget and Forget (2016) suggested that DDS sediment ejections induced by IIBS repeatedly recur from the same vent in a given season and result in fluidized, viscous debris flows, perhaps beneath the slab ice. Dark sand likely was eroded by CO_2 gas en route to the vents, and these dendritic, araneiform troughs plus downslope flows may rework the sub-ice dune surface and carve the small tributary channels that merge downslope and empty into the linear dune gullies. The polygonal network of cracks in the ice remains clearly visible until L_s 157° or later (MY28, MY31) when ice thickness is ~0.33–0.49 m based on model estimates (Figures 2, S1k, and S2c). Increasing insolation and subsequent ice brightening (Paige, 1985) typically conceals polygonal cracks thereafter, but araneiform troughs in the same area become more visible (Figures 2 and S1k). DDS form repeatedly at the same spatial locations having positive relief year after year, indicating a positive-feedback mechanism for the vents, such that they are a self-reinforcing phenomenon. After all frost has sublimated (L_s 217°+; Figure S2c), dendritic, araneiform troughs/furrows and positive-relief knobs (Gardin et al., 2010) upon which DDS vents annually form and link up remain visible. The positive-relief knobs may be deposits of material that was funneled toward the vent but not yet ejected.

3. CO_2 Ice Blocks: Their Formation and Dust Content

Using the KRC thermal model (Kieffer, 2013; see Text S2), we estimated the end-of-season CO_2 ice-thickness distribution on the Russell crater megadune within the digital terrain model (DTM) footprint (Figure 4a). By L_s 202°, the model predicts a directly condensed CO_2 ice maximum accumulation thickness of 0.50 m on the steepest slopes. However, alcoves are typically a few meters deep and also amass windblown CO_2 snow (Figure 3a). Snow morphs into porous ice on Mars (Cornwall & Titus, 2009, 2010; Mount & Titus, 2015), so CO_2 ice within alcoves (both directly deposited plus metamorphosed snow) is likely to be several meters

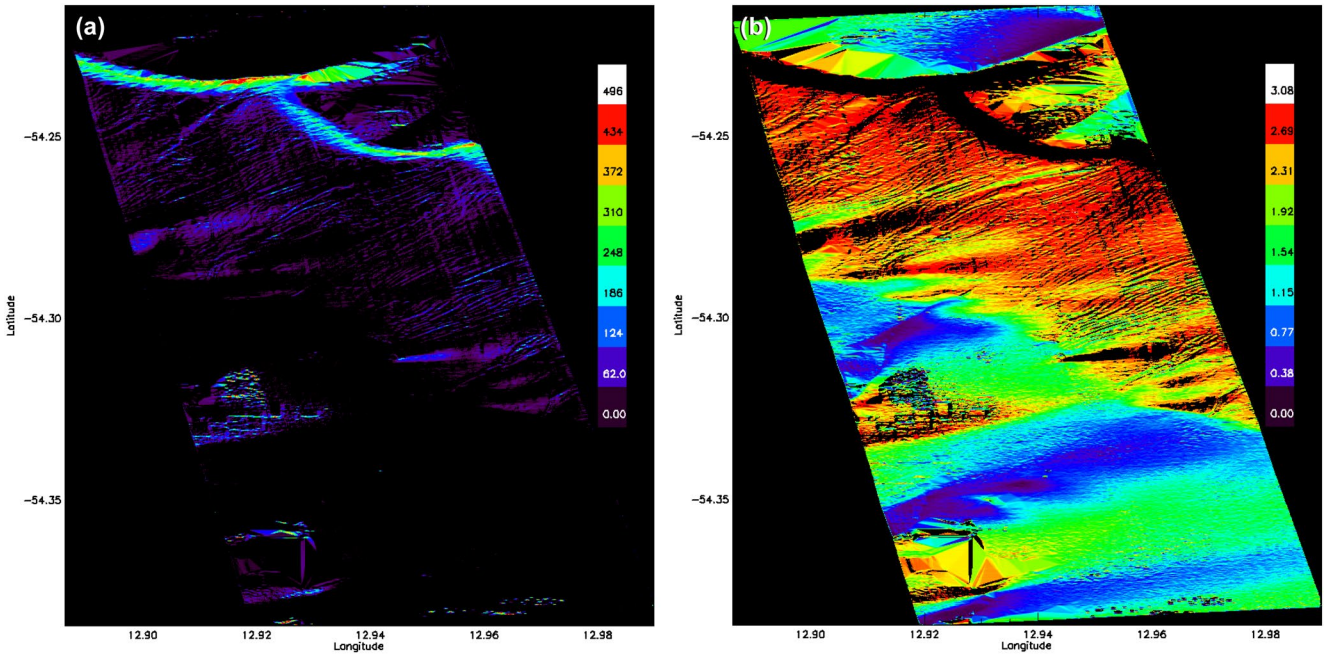

Figure 4. Modeled CO_2 ice and dust thicknesses at L_s 202° within the DTM footprint. North is up. (a) KRC thermal model of CO_2 ice thickness (mm, assuming ice density of 1,000 kg/m^3, see Text S2). The KRC thermal model outputs CO_2 ice thickness at local midnight. Therefore, a residual ~10–15-mm-thick CO_2 ice layer would sublime completely during daylight hours. (b) Estimated dust thickness (microns) comprising seasonal sublimation lag. Areas with CO_2 ice coverage are color-coded black because sublimation lag remains covered by CO_2 ice. DTM, digital terrain model.

thick. We measured 1.5- to 5-m CO_2 ice blocks at rest in Russell crater megadune gully channels (Figures S1c and S1l), indicating that even larger blocks detached from their point of origin and slid downhill. We hypothesize that IIBS drives recurrent jets of CO_2 gas upward through vents in the slab ice, ultimately dislodging CO_2 ice blocks that potentially were discretized by vigorous agitation of the polygonal crack network in the slab ice observed earlier in the season (Figure 3).

Accounting for windblown snow, in addition to atmospherically condensed CO_2 frost, increases the likely dust content of the coalesced alcove ice deposit because atmospheric dust commonly forms condensation nuclei for CO_2 snow. Assuming an atmospheric dust-to-gas mixing ratio of 7.5×10^{-6} (Kieffer, 2007) and a CO_2-ice density of 1,000 kg/m^3 (Aharonson et al., 2004; Haberle et al., 2004; Kieffer et al., 2000; Matsuo & Heki, 2009; Mount & Titus, 2015; Smith et al., 2001; Text S2), the dust abundance in a 2-m-thick ice block would be 15 μm/m^2. A 2-m-thick ice block with greater density, which is possible due to annealing, or an even larger block would have greater dust abundance. Based on these assumptions, we estimated the end-of-season, dust-thickness distribution (comprising a seasonal sublimation lag) at L_s 202° on the Russell crater megadune within the DTM footprint (Figure 4b).

4. Mobility of CO_2 Ice Blocks

By L_s 197° (MY28) and possibly earlier, gas pressure from IIBS can break the slab ice, dislodge and push discrete CO_2 ice blocks out of place, such that they fall from alcoves or adjacent steep terrain and funnel into linear dune gullies, down which they slide (Figures 1f, 1h, and 3d). Experimental studies of CO_2 ice blocks (i.e., dry ice) sliding down terrestrial sand dune slopes (Diniega et al., 2013) have shown that the sliding block sublimes from all sides, providing a low-friction gas cushion between the block and the dune slope.

Two airborne dust plumes lofted at L_s 202° (MY33) are observed in CTX image J06_047078_1253 (Figure 1), and part of the near-field plume is also observed at 25-cm resolution in the simultaneously acquired HiRISE image ESP_047078_1255 (Figure 1h). We subsequently identified two additional images of airborne plumes on the same megadune slope (HiRISE PSP_002904_1255 and CTX D06_029408_1254) at L_s 197° (MY28) and L_s 200° (MY31; Figures 1f and 1g).

The Russell crater megadune seasonally accumulates a coarse silt/dust layer of CO_2-ice sublimation-lag residue that is a few microns thick by L_s 202°, based on our modeling (Figure 4b). Gas pressure from subliming, sliding CO_2 ice blocks redistributes sublimation lag, potentially clearing coarse silt from levees surrounding dune gully channels and depositing bright silt fringes around recently active channels (e.g., note the albedo variations in Figures 1h and S1h). Dark gully fringes (Dundas et al., 2012), where present (e.g., Figure S1c), may develop when sliding, off-gassing ice blocks throw low-albedo sand out of channels via saltation and onto surrounding levees, burying bright sublimation lag beneath a fresh deposit of sand. Bright gully fringes result when saltating coarse silt driven by the off-gassing pressure of ice blocks is redeposited farther from the channel; locally thick silt deposits may form adjacent to recently active gullies, visible as an intermediate-albedo fringe surrounding gullies in optical data (Figure S1l). As dust is mobilized by sliding, subliming blocks of CO_2 ice, finer grains are lofted into suspension, thus forming optically thick, narrow dust plumes that are dispersed downwind (Figure 3e). Although mobile ice blocks cannot be observed at the source of the optically thick plumes because they are hidden by their own clouds of debris, the narrowness of the plumes originating inside gullies indicates ice-block point sources (Figures 1f–1h and S1h′), not clouds of avalanching sand and frost that were identified in the northern hemisphere by others (Hansen et al., 2011; Russell et al., 2008). We also rule out an interpretation that the plumes occurring between L_s 197° and 202° are a manifestation of local DDS venting on the lee slope (Hansen et al., 2020), because slab ice has largely sublimed from their gully point sources by this time of year (e.g., Figure 4a).

5. The Fate of CO_2 Ice Blocks

CO_2 ice blocks will come to rest when gas lubrication is no longer sufficient to overcome friction, such as when the slope of the gully flattens, as occurs near the base of the lee slope. Subliming blocks will redistribute adjacent coarse silt to a larger area, as well as add their own embedded coarse-grained dust to the surroundings in the visible form of an intermediate-albedo dust fringe around linear dune gullies and the

final resting places of ice blocks (e.g., Figures 1 and S1a). The presence of multiple ice blocks at rest near the terminus of gullies within the same dust-plume imagery (e.g., Figure S1l) provides additional support for our interpretation of the airborne plumes.

Increasing CO_2 ice surface albedo with increasing insolation has been observed (Paige, 1985; Paige & Ingersoll, 1985). An ice block likely will brighten from albedo 0.3 to 0.7. When an ice block is dislodged from its point of origin, the ice block surface can become thermally stressed due to a sudden change in its surface thermal gradient (especially if the surface had been previously in contact with a cold, sheltered alcove and then became exposed to the warmer atmosphere; Kieffer, 1968) and/or due to an increased exposure to insolation (Paige, 1985; Paige & Ingersoll, 1985); translucent CO_2 ice will fracture and brighten due to increased internal scattering. Ice brightening (i.e., increased albedo) reduces the sublimation rate and increases the longevity of an ice block. HiRISE image ESP_047078_1255 captured several three-dimensional-appearing, high-albedo features at rest in linear gullies (Figures 1b, S1c, and S1l) that are visually consistent with CO_2 ice blocks. As CO_2 ice blocks slowly sublimate, they may leave a patchy frost residue before disappearing completely (Figures 1b and S1c).

6. Implications of CO_2 Ice Blocks

A combination of optical and spectral imaging, stereo-image-derived DTMs, and observation-validated models provides new insights into CO_2-ice-block formation, mobility, and final disposition. We bring together an 11-Mars-year baseline of mission data and thermal modeling to construct a compelling and consistent story that vent-dislodged, sliding CO_2 ice blocks are an agent of change on the Russell crater megadune. Using the KRC thermal model, we have estimated the spatiotemporal distribution of CO_2 ice thickness at key locations and times (Figures 4a and S2e–S2j). We then used our model-based estimates of CO_2 ice thickness to estimate the thickness of seasonal sublimation lag (coarse-grained silt; Figure 4b), whose redistribution by sliding and subliming blocks of CO_2 ice explains many of the observed albedo features (e.g., dune gully fringes) on the lee slope after most of the CO_2 ice has sublimed. Previously, sliding CO_2 ice blocks were suggested to have formed the Russell crater linear dune gullies, but our additional observations and modeling have strongly enhanced the likelihood that this uniquely Martian process is responsible for many of the albedo variations observed this time of year on the Russell megadune lee slope, as well as on smaller dunes within this crater. CO_2 ice blocks are actively modifying the surface of Mars, altering linear dune gullies and redistributing coarse-grained dust and silt (seasonal sublimation lag).

Data Availability Statement

JMARS (https://jmars.asu.edu/), a geospatial information system, was used to identify the Mars imagery and data used in this research study, which are publicly available through NASA's Planetary Data System (https://pds-geosciences.wustl.edu/missions/mep/index.htm) and may be found online at http://viewer.mars.asu.edu/ using the cited image numbers. The KRC thermal modeling code may be accessed via links in the KRC Wiki at http://krc.mars.asu.edu/.

Acknowledgments
This research study was conducted at Southwest Research Institute, in San Antonio, Texas, and at the U.S. Geological Survey, Astrogeology Science Center, in Flagstaff, Arizona. Federal research funding was granted by the NASA Mars Data Analysis Program, Grant Nos. 80NSSC19K1595 (Dinwiddie) and 80HQTR19T0103 (Titus). This study benefitted from insightful review comments by Colin Dundas, Oded Aharonson and an anonymous reviewer. This study also benefited from related dialog the authors had with David Stillman and Kenneth Herkenhoff. Dr. Dinwiddie expresses her gratitude for GIS support provided by Taylor Holt.

References

Aharonson, O. (2004). Sublimation at the base of a seasonal CO_2 slab on Mars. In *35th Lunar and Planetary Science Conference, March 15–19, 2004*. League City, TX. Abstract No. 1918. Available at www.lpi.usra.edu/meetings/lpsc2004/pdf/1918.pdf

Aharonson, O., Zuber, M. T., Smith, D. E., Neumann, G. A., Feldman, W. C., & Prettyman, T. H. (2004). Depth, distribution, and density of CO_2 deposition on Mars. *Journal of Geophysical Research*, *109*, E05004. https://doi.org/10.1029/2003JE002223

Auld, K. S., & Dixon, J. C. (2016). A classification of Martian gullies from HiRISE imagery. *Planetary and Space Science*, *131*, 88–101. https://doi.org/10.1016/j.pss.2016.08.002

Ceamanos, X., Douté, S., Luo, B., Schmidt, F., Jouannic, G., & Chanussot, J. (2011). Intercomparison and validation of techniques for spectral unmixing of hyperspectral images: A planetary case study. *IEEE Transactions on Geoscience and Remote Sensing*, *49*, 4341–4358. https://doi.org/10.1109/TGRS.2011.2140377

Christensen, P. R., Anderson, D. L., Chase, S. C., Clark, R. N., Kieffer, H. H., Malin, M. C., et al. (1992). Thermal emission spectrometer experiment: Mars observer mission. *Journal of Geophysical Research*, *97*, 7719–7734. https://doi.org/10.1029/92JE00453

Christensen, P. R., Bandfield, J. L., Hamilton, V. E., Ruff, S. W., Kieffer, H. H., Titus, T. N., et al. (2001). Mars global surveyor thermal emission spectrometer experiment: Investigation description and surface science results. *Journal of Geophysical Research*, *106*, 23823–23871. https://doi.org/10.1029/2000JE001370

Christensen, P. R., Jakosky, B. M., Kieffer, H. H., Malin, M. C., McSween, H. Y., Jr., Nealson, K., et al. (2004). The Thermal Emission Imaging System (THEMIS) for the Mars 2001 Odyssey Mission. *Space Science Reviews*, *110*, 85–130. https://doi.org/10.1023/B:SPAC.0000021008.16305.94

Cornwall, C., & Titus, T. N. (2009). Spatial and temporal distributions of Martian north polar cold spots before, during, and after the global dust storm of 2001. *Journal of Geophysical Research*, *114*, E02003. https://doi.org/10.1029/2008JE003243

Cornwall, C., & Titus, T. N. (2010). A comparison of Martian north and south polar cold spots and the long-term effects of the 2001 global dust storm. *Journal of Geophysical Research*, *115*, E06011. https://doi.org/10.1029/2009JE003514

Costard, F., Forget, F., Mangold, N., & Peulvast, J. P. (2002). Formation of recent Martian debris flows by melting of near-surface ground ice at high obliquity. *Science*, *295*, 110–113. https://doi.org/10.1126/science.1066698

Diniega, S. (2014). Linear gullies (Mars). In H. Hargitai, & Á. Kereszturi (Eds.), *Encyclopedia of planetary landforms* (pp. 1–5). New York, NY: Springer.

Diniega, S., Hansen, C. J., McElwaine, J. N., Hugenholtz, C. H., Dundas, C. M., McEwen, A. S., & Bourke, M. C. (2013). A new dry hypothesis for the formation of Martian linear gullies. *Icarus*, *225*, 526–537. https://doi.org/10.1016/j.icarus.2013.04.006

Dundas, C. M., Diniega, S., Hansen, C. J., Byrne, S., & McEwen, A. S. (2012). Seasonal activity and morphological changes in Martian gullies. *Icarus*, *220*, 124–143. https://doi.org/10.1016/j.icarus.2012.04.005

Dundas, C. M., McEwen, A. S., Diniega, S., Hansen, C. J., Byrne, S., & McElwaine, J. N. (2019). The formation of gullies on Mars today. In S. J. Conway, J. L. Carrivick, P. A. Carling, T. De Haas, & T. N. Harrison (Eds.), *Martian Gullies and Their Earth Analogs* (Vol. 467, pp. 67–94). London: Geological Society, London, Special Publicaion.

Gardin, E., Allemand, P., Quantin, C., & Thollot, P. (2010). Defrosting, dark flow features, and dune activity on Mars: Example in Russell crater. *Journal of Geophysical Research*, *115*, E06016. https://doi.org/10.1029/2009JE003515

Haberle, R. M., Mattingly, B., & Titus, T. N. (2004). Reconciling different observations of the CO_2 ice mass loading of the Martian north polar cap. *Geophysical Research Letters*, *31*, L05702. https://doi.org/10.1029/2004GL019445

Hansen, C. J., Bourke, M., Bridges, N. T., Byrne, S., Colon, C., Diniega, S., et al. (2011). Seasonal erosion and restoration of Mars' northern polar dunes. *Science*, *331*, 575–578. https://doi.org/10.1126/science.1197636

Hansen, C. J., Conway, S., Portyankina, G., Thomas, N., McEwen, A., & Perry, J. (2020). Searching for seasonal jets on Mars in Cassis and HiRISE images. In *51st Lunar and Planetary Science Conference*. Abstract No. 2351. Available at www.hou.usra.edu/meetings/lpsc2020/pdf/2351.pdf

Hansen, C. J., Thomas, N., Portyankina, G., McEwen, A., Becker, T., Byrne, S., et al. (2010). HiRISE observations of gas sublimation-driven activity in Mars' southern polar regions: I. Erosion of the surface. *Icarus*, *205*, 283–295. https://doi.org/10.1016/j.icarus.2009.07.021

Jouannic, G., Conway, S. J., Gargani, J., Costard, F., Massé, M., Bourgeois, O., et al. (2018). Morphological characterization of landforms produced by springtime seasonal activity on Russell crater megadune (Vol. 467, pp. 115–144). London: Geological Society, London, Special Publication. https://doi.org/10.1144/SP467.16

Jouannic, G., Gargani, J., Conway, S. J., Costard, F., Balme, M. R., Patel, M. R., et al. (2015). Laboratory simulation of debris flows over sand dunes: Insights into gully-formation (Mars). *Geomorphology*, *231*, 101–115. https://doi.org/10.1016/j.geomorph.2014.12.007

Jouannic, G., Gargani, J., Costard, F., Ori, G. G., Marmo, C., Schmidt, F., & Lucas, A. (2012). Morphological and mechanical characterization of gullies in a periglacial environment: The case of the Russell crater dune (Mars). *Planetary and Space Science*, *71*, 38–54. https://doi.org/10.1016/j.pss.2012.07.005

Kieffer, H. H. (1968). *Near infrared spectral reflectance of simulated Martian frosts* (Ph.D. Dissertation). California Institute of Technology. https://doi.org/10.7907/BHED-BJ17

Kieffer, H. H. (2007). Cold jets in the Martian polar caps. *Journal of Geophysical Research*, *112*(E8), E08005. https://doi.org/10.1029/2006JE002816

Kieffer, H. H. (2013). Thermal model for analysis of Mars infrared mapping. *Journal of Geophysical Research: Planets.*, *118*, 451–470. https://doi.org/10.1029/2012JE004164

Kieffer, H. H., Titus, T. N., Mullins, K. F., & Christensen, P. R. (2000). Mars south polar spring and summer behavior observed by TES: Seasonal cap evolution controlled by frost grain size. *Journal of Geophysical Research*, *105*, 9653–9699. https://doi.org/10.1029/1999JE001136

Malin, M. C., Bell, J. F., III, Cantor, B. A., Caplinger, M. A., Calvin, W. M., Clancy, R. T., et al. (2007). Context camera investigation on board the Mars reconnaissance orbiter. *Journal of Geophysical Research*, *112*, E05S04. https://doi.org/10.1029/2006JE002808

Malin, M. C., Danielson, G. E., Ingersoll, A. P., Masursky, H., Veverka, J., Ravine, M. A., & Soulanille, T. A. (1992). Mars observer camera. *Journal of Geophysical Research*, *97*, 7699–7718. https://doi.org/10.1029/92JE00340

Malin, M. C., & Edgett, K. S. (2001). Mars Global Surveyor Mars orbiter camera: Interplanetary cruise through primary mission. *Journal of Geophysical Research*, *106*, 23429–23570. https://doi.org/10.1029/2000JE001455

Malin, M. C., Edgett, K. S., Cantor, B. A., Caplinger, M. A., Danielson, G. E., Jensen, E. H., et al. (2010). An overview of the 1985–2006 Mars orbiter camera science investigation. *Mars*, *5*, 1–60. https://doi.org/10.1555/mars.2010.0001

Mangold, N., Costard, F., & Forget, F. (2003). Debris flows over sand dunes on Mars: Evidence for liquid water. *Journal of Geophysical Research*, *108*, 5027. https://doi.org/10.1029/2002JE001958

Mangold, N., Mangeney, A., Migeon, V., Ansan, V., Lucas, A., Baratoux, D., & Bouchut, F. (2010). Sinuous gullies on Mars: Frequency, distribution, and implications for flow properties. *Journal of Geophysical Research*, *115*, E11001. https://doi.org/10.1029/2009JE003540

Matsuo, H., & Heki, K. (2009). Seasonal and inter-annual changes of volume density of Martian CO_2 snow from time-variable elevation and gravity. *Icarus*, *202*, 90–94. https://doi.org/10.1016/j.icarus.2009.02.023

McEwen, A. S., Eliason, E. M., Bergstrom, J. W., Bridges, N. T., Hansen, C. J., Delamere, W. A., et al. (2007). Mars reconnaissance orbiter's high resolution imaging science experiment (HiRISE). *Journal of Geophysical Research*, *112*, E05S02. https://doi.org/10.1029/2005JE002605

McKeown, L. E., Bourke, M. C., & McElwaine, J. N. (2017). Experiments on sublimating carbon dioxide ice and implications for contemporary surface processes. *Scientific Reports*, *7*, 14181. https://doi.org/10.1038/s41598-017-14132-2

Miyamoto, H., Dohm, J. M., Baker, V. R., Beyer, R. A., & Bourke, M. (2004). Dynamics of unusual debris flows on Martian sand dunes. *Geophysical Research Letters*, *31*, L13701. https://doi.org/10.1029/2004GL020313

Mount, C. P., & Titus, T. N. (2015). Evolution of Mars' northern polar seasonal CO_2 deposits: Variations in surface brightness and bulk density. *Journal of Geophysical Research: Planets 120*, 1252–1266. https://doi.org/10.1002/2014JE004706

Murchie, S., Arvidson, R., Bedini, P., Beisser, K., Bibring, J.-P., Bishop, J., et al. (2007). Compact Reconnaissance imaging spectrometer for Mars (CRISM) on Mars reconnaissance orbiter (MRO). *Journal of Geophysical Research*, *112*, E05S03. https://doi.org/10.1029/2006JE002682

Paige, D. A. (1985). *The annual heat balance of the Martian polar caps from Viking observations* (Ph.D. Thesis). California Institute of Technology

Paige, D. A., & Ingersoll, A. P. (1985). Annual heat-balance of Martian polar caps: Viking observations. *Science*, *228*, 1160–1168. https://doi.org/10.1126/science.228.4704.1160

Pasquon, K., Gargani, J., Massé, M., & Conway, S. J. (2016). Present-day formation and seasonal evolution of linear dune gullies on Mars. *Icarus*, *274*, 195–210. https://doi.org/10.1016/j.icarus.2016.03.024

Pilorget, C., & Forget, F. (2016). Formation of gullies on Mars by debris flows triggered by CO_2 sublimation. *Nature Geoscience*, *9*, 65–69. https://doi.org/10.1038/ngeo2619

Piqueux, S., & Christensen, P. R. (2008). North and south subice gas flow and venting of the seasonal caps of Mars: A major geomorphological agent. *Journal of Geophysical Research*, *113*, E06005. https://doi.org/10.1029/2007JE003009

Portyankina, G. (2014). Araneiform. In H. Hargitai, & Á. Kereszturi (Eds.), *Encyclopedia of planetary landforms* (pp. 1–7). New York, NY: Springer.

Portyankina, G., Hansen, C. J., & Aye, K.-M. (2017). Present-day erosion of Martian polar terrain by the seasonal CO_2 jets. *Icarus*, *282*, 93–103. https://doi.org/10.1016/j.icarus.2016.09.007

Reiss, D., Erkeling, G., Bauch, K. E., & Hiesinger, H. (2010). Evidence for present day gully activity on the Russell crater dune field, Mars. *Geophysical Research Letters*, *37*, L06203. https://doi.org/10.1029/2009GL042192

Reiss, D., & Jaumann, R. (2003). Recent debris flows on Mars: Seasonal observations of the Russell Crater dune field. *Geophysical Research Letters*, *30*, 1321. https://doi.org/10.1029/2002GL016704

Russell, P., Thomas, N., Byrne, S., Herkenhoff, K., Fishbaugh, K., Bridges, N., et al. (2008). Seasonally active frost-dust avalanches on a north polar scarp of Mars captured by HiRISE. *Geophysical Research Letters*, *35*, L23204. https://doi.org/10.1029/2008GL035790

Smith, D. E., Zuber, M. T., & Neumann, G. A. (2001). Seasonal variations of snow depth on Mars. *Science*, *294*, 2141–2145. https://doi.org/10.1126/science.1066556

Védie, E., Costard, F., Font, M., & Lagarde, J. L. (2008). Laboratory simulations of Martian gullies on sand dunes. *Geophysical Research Letters*, *35*, L21501. https://doi.org/10.1029/2008GL035638

Reference From the Supporting Information

Kirk, R. L., Howington-Kraus, E., Rosiek, M. R., Anderson, J. A., Archinal, B. A., Becker, K. J., et al. (2008). Ultrahigh resolution topographic mapping of Mars with MRO HiRISE stereo images: Meter-scale slopes of candidate Phoenix landing sites. *Journal of Geophysical Research*, *113*, E00A24. https://doi.org/10.1029/2007JE003000